Supporting Information

Partially reversible H_2S adsorption by MFM-300(Sc): Formation of polysulfides

J. Gabriel Flores,[#,†,‡] J. Antonio Zárate-Colín,[#,†,§] Elí Sánchez-González,[†,Ŧ] Jorge R. Valenzuela,[Λ] Aída Gutiérrez-Alejandre,[*,Λ] Jorge Fernando Ramírez-Solís,[Λ] Vojtech Jancik,[ó,ђ] Julia Aguilar-Pliego,[‡] Maria Cristina Zorrilla,[Ц] Hugo A. Lara-García,[Ц] Eduardo González-Zamora,[Ъ] Gregorio Guzmán-González,[Ъ] Ignacio González,[Ъ] Guillaume Maurin,[*,§] and Ilich A. Ibarra[*,†]

[†]Laboratorio de Fisicoquímica y Reactividad de Superficies (LaFReS), Instituto de Investigaciones en Materiales, Universidad Nacional Autónoma de México, Circuito Exterior s/n, CU, Del. Coyoacán, 04510, Ciudad de México, Mexico.

[‡]UAM-Azcapotzalco, San Pablo 180, Col. Reynosa-Tamaulipas, Azcapotzalco, C.P. 02200, Ciudad de México, Mexico.

[§]Institut Charles Gerhardt Montpellier, UMR-5253, Université de Montpellier, CNRS, ENSCM, Place E. Bataillon, 34095 Montpellier cedex 05, France.

[Λ]UNICAT, Departamento de Ingeniería Química, Facultad de Química, Universidad Nacional Autónoma de México (UNAM), Coyoacán, Ciudad de México, Mexico.

[ó]Centro Conjunto de Investigación en Química Sustentable UAEM-UNAM, Carr. Toluca-Atlacomulco Km 14.5, Toluca, Estado de México 50200, México. Personal del Instituto de Química de la UNAM.

[Ц]Instituto de Física, Universidad Nacional Autónoma de México, Circuito de la Investigación científica s/n, CU, Del. Coyoacán, 04510, Ciudad de México, Mexico.

[Ъ]Departamento de Química, Universidad Autónoma Metropolitana-Iztapalapa, San Rafael Atlixco 186, Col. Vicentina, Iztapalapa, C. P. 09340, Ciudad de México, Mexico.

[Ŧ]Institute for Integrated Cell-Material Sciences (WPI-iCeMS), Kyoto University, Yoshida, Sakyo-ku, Kyoto 606-8501, Japan.

[ђ]Universidad Nacional Autónoma de México, Instituto de Química, Ciudad Universitaria, Ciudad de México, 04510, México.

Corresponding Authors

* E-mail: aidag@unam.mx
* E-mail: guillaume.chastanet@icmcb.cnrs.fr
* E-mail: argel@unam.mx

[#]These authors contributed equally.

1. Crystal Structure of MFM-300(Sc)

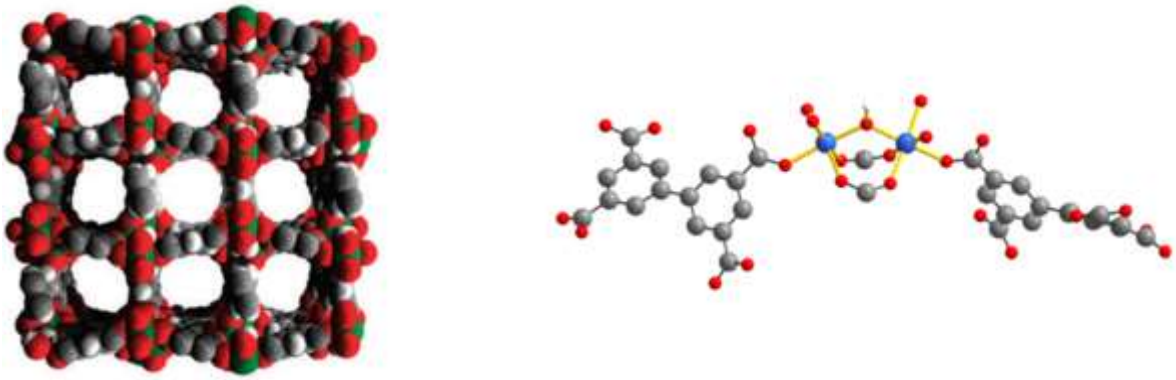

Figure S1. (left) space-filling view of the structure of MFM-300(Sc) along the b-axis showing 8.1 Å channels (Reproduced from[1] with permission from The Royal Society of Chemistry); and (right) view of the coordination at Sc(III) in MFM-300(Sc), showing $[BPTC]^{4-}$ and the μ_2-OH group (Reproduced from[2] with permission from The American Chemical Society).

2. Experimental

Synthesis of MFM-300(Sc)

The material was synthesised using a method previously reported by Ibarra *et al.*[1]: a mixture of scandium triflate (0.061 mmol) and H_4BPTC (0.010 g) in THF (4.0 ml), DMF (3.0 ml), water (1.0 ml) and HCl (36.5%, 2 drops). The solution was then placed in a pressure tube and heated in an oil bath to 75 °C for 72 h. The tube was cooled down to room temperature at a rate of 0.1 °C/min, and the colourless crystalline product was separated by filtration, washed several times with acetone.

Synthesis of MFM-300(In)

The material was synthesised using a method previously reported by Hong *et al.*[3]: a mixture of Indium(III) nitrate hydrate (0.40 mmol) and H_4BPTC (0.10 mmol) in DMF (5 ml), CH_3CN (5 ml) and HNO_3 (65 wt %, 0.2 ml). The solution was then placed in a pressure tube and heated in an oil bath to 85 °C for 72 h. The tube was cooled down to room temperature at a rate of 0.1 °C/min, and the colourless crystalline product was separated by filtration, washed several times with acetone.

Powder X-ray diffraction (PXRD)

Patterns were collected in Bragg-Brentano geometry with Cu-Kα1 radiation (λ = 1.540562 Å) on a Rigaku ULTIMA IV. The powder patterns were recorded from 5 to 40° (2θ) in 0.02° steps and a scan rate of 0.2°/min.

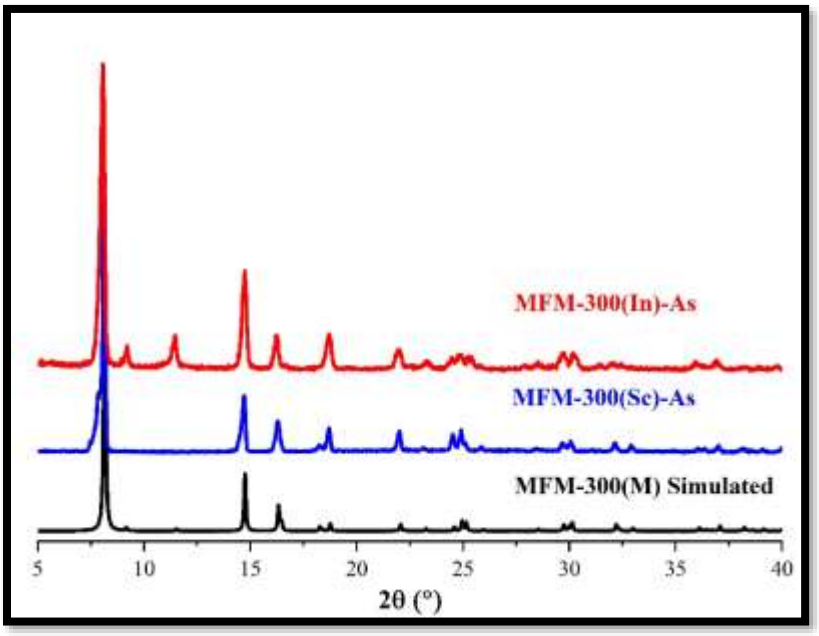

Figure S2. PXRD of MFM-300(Sc) simulated (black) and as synthesised (blue).

Adsorption isotherms for N_2

N_2 isotherms were performed on a Belsorp mini II analyser under vacuum (10^{-3} bar). Samples of MFM-300(Sc) and MFM-300(In) were activated at 180 °C for two hours (under vacuum, 10^{-3} bar). N_2 adsorption isotherms for each activated material, at 77 K, were performed to estimate BET surface areas ($0.01 < P/P_0 < 0.04$).

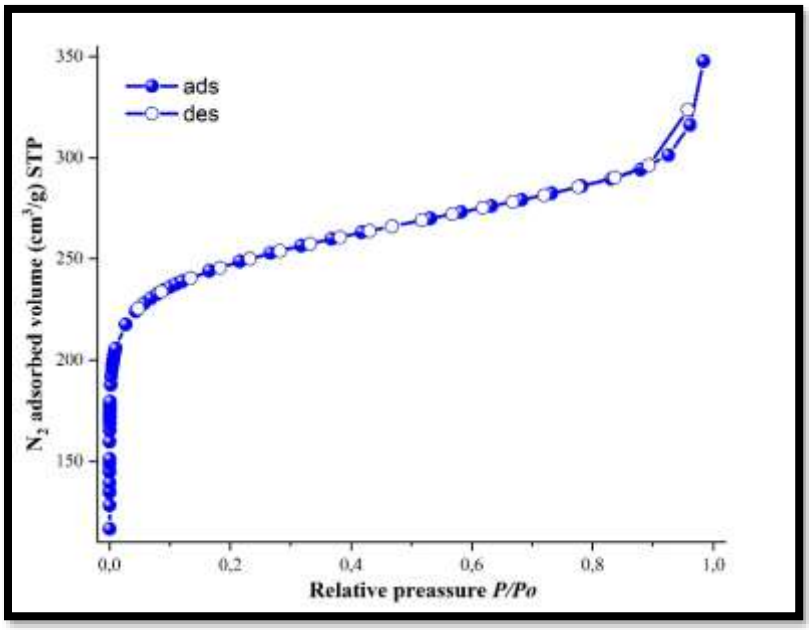

Figure S3. N_2 isotherm of MFM-300(Sc)-As.

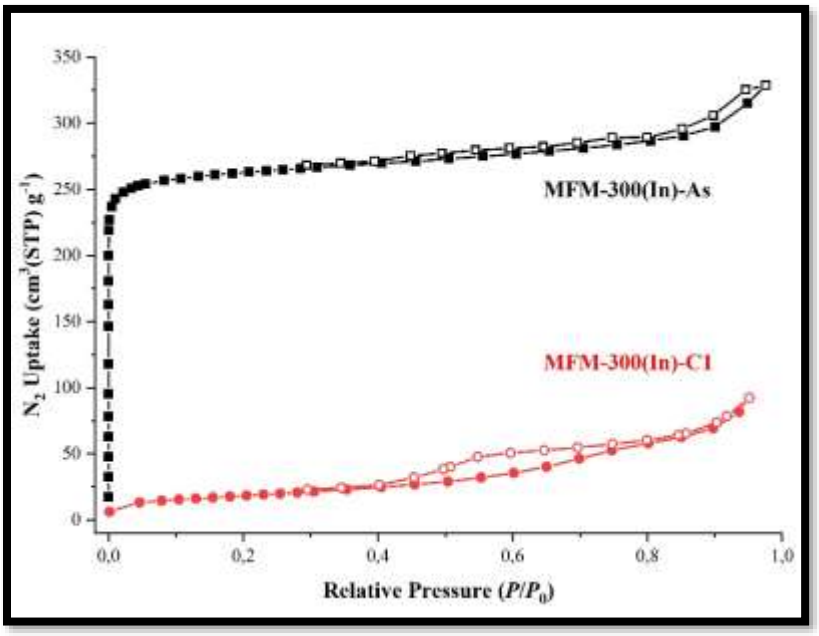

Figure S4. N_2 isotherm of MFM-300(In)-As (before H_2S uptake) and C1 (after H_2S uptake).

H_2S Breakthrough experiments

H_2S experiments were made using a HP 5890 GC, by continuous injections of the system exhaust, of each injection we obtained a chromatogram. From the corresponding chromatogram we integrate the H_2S signal to obtain its quantity. Knowing the H_2S concentration from the feed, we can calculate the H_2S concentration in each one of the injections, as the saturation concentration is the original feed concentration. Dynamic breakthrough experiments were carried out in a home-made system (Scheme S1).

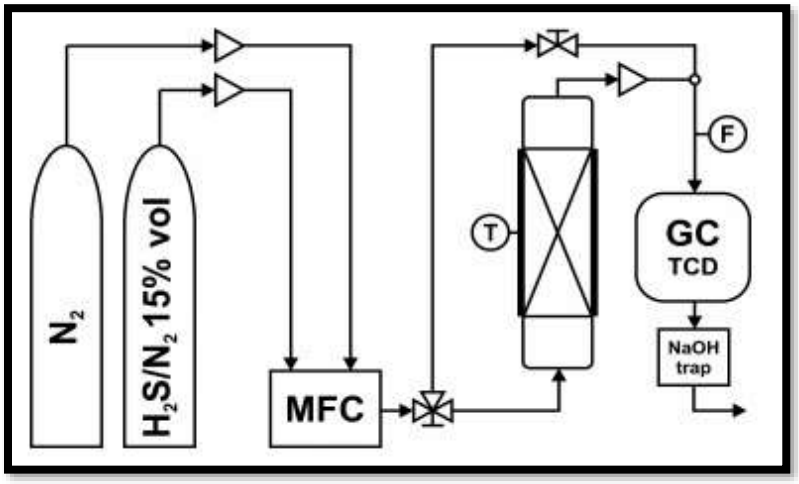

Scheme S1. Representation of breakthrough dynamic system for H_2S uptake experiments.

Each sample was activated in situ at 180 °C for 2 hours with a constant flow of dry N_2 (25 mL/min, ultrapure grade (99.98%) N_2 gas (Praxair)) and then slowly cooled to 25 °C. Then the H_2S concentration was adjusted with a mass flow controller fed with two lines: dry N_2 and H_2S/N_2 15 %vol, the gas concentration used for the H_2S experiments was 10% of H_2S with a flow of 25 ml/min. The breakthrough experiments were carried out at 25 °C and the downstream flow was analysed with a GC. The reactivation of the sample was at 25 °C for 15 minutes under a flow of dry N_2 (25 ml/min).

The H_2S adsorption capacity for each cycle was calculated using Eq. S1, where *'V_{H2S}'* represents the H_2S volumetric capacity ($cm^3\ g^{-1}$), *'m'* the adsorbent mass (g), *'F'* the input flow rate ($cm^3\ min^{-1}$), *'Cf'* and *'Ct'* the influent and downstream H_2S concentrations respectively (% vol), and *'t'* the time (min)[4].

$$V_{H_2S} = \frac{F}{C_f m} \cdot \int_0^t \left(C_f - C_t\right) dt \qquad \textbf{Eq. S1}$$

As mentioned before, the adsorption column has a porous glass bed thus, a blank run before each experiment was measured to eliminate the adsorption contribution of the column. In Figure S6 the black circles represent the adsorption of the column, and the others circles represent the MOF adsorption for each cycle. Then the MFM-300(Sc) corrected volumetric capacity '$V_{H2S,corr}$' was estimated using Eq. S2 for each cycle, for MFM-300(In) was just one cycle.

$$V_{H_2S,corr} = V_{H_2S,blank} - V_{H_2S,sample} \qquad \textbf{Eq. S2}$$

The H_2S adsorption capacity is often reported as *'q_{H2S}'* (mol g^{-1}), this value was roughly estimated with the volumetric adsorption capacity '$V_{H2S,corr}$' ($cm^3\ g^{-1}$) and the ideal gas law Eq. S3. Where *'p'* is the system pressure (77.3 kPa), *'T'* the measurement temperature (298 K), and *'R'* the ideal gas constant (8314.4598 cm^3 kPa K^{-1} mol^{-1}).

$$q_{H_2S} = \frac{V_{H_2S,corr} \cdot p}{R \cdot T} \qquad \textbf{Eq. S3}$$

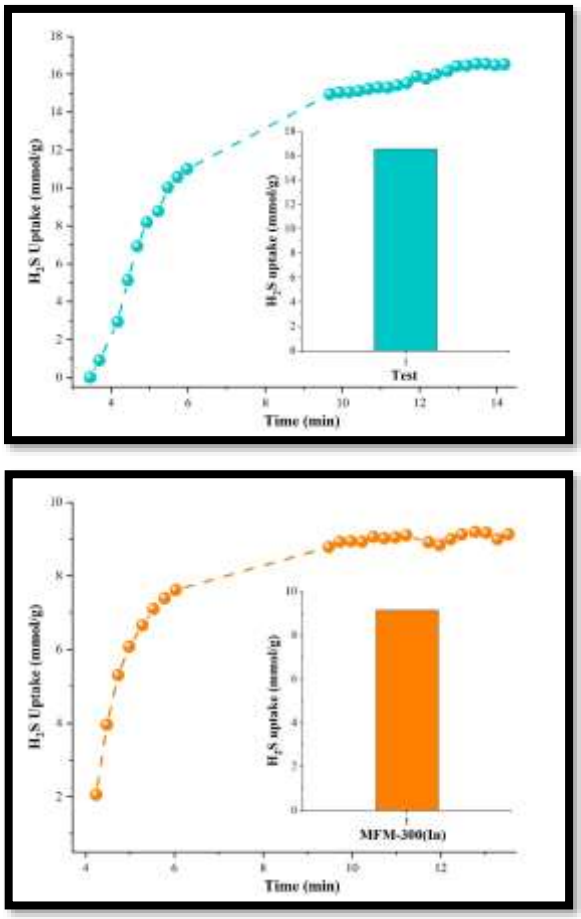

Figure S5. First H_2S breakthrough experiments for: (top, a) MFM-300(Sc) and (bottom, b) MFM-300(In).

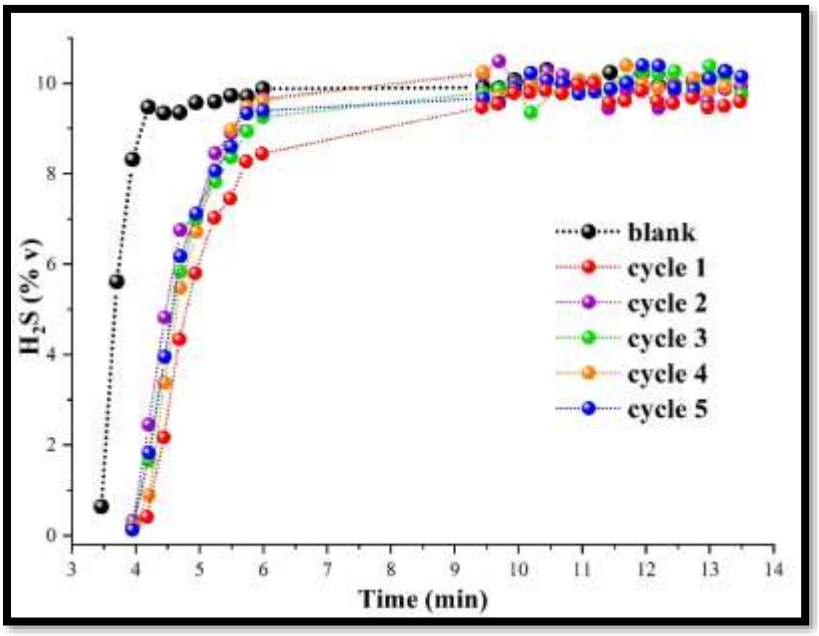

Figure S6. Consecutive MFM-300(Sc) breakthrough of H_2S experiment.

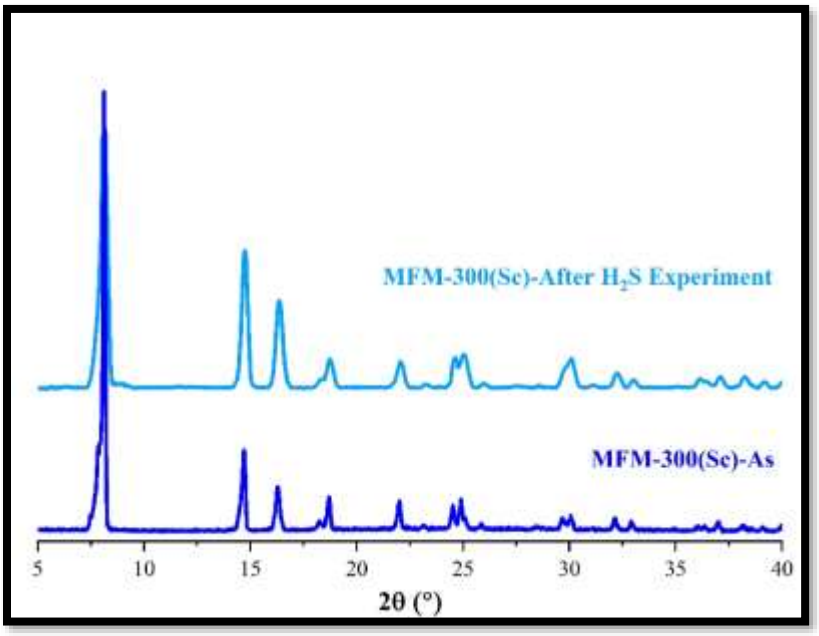

Figure S7. PXRD of MFM-300(Sc) after H_2S experiment (light blue) and as synthesised (dark blue).

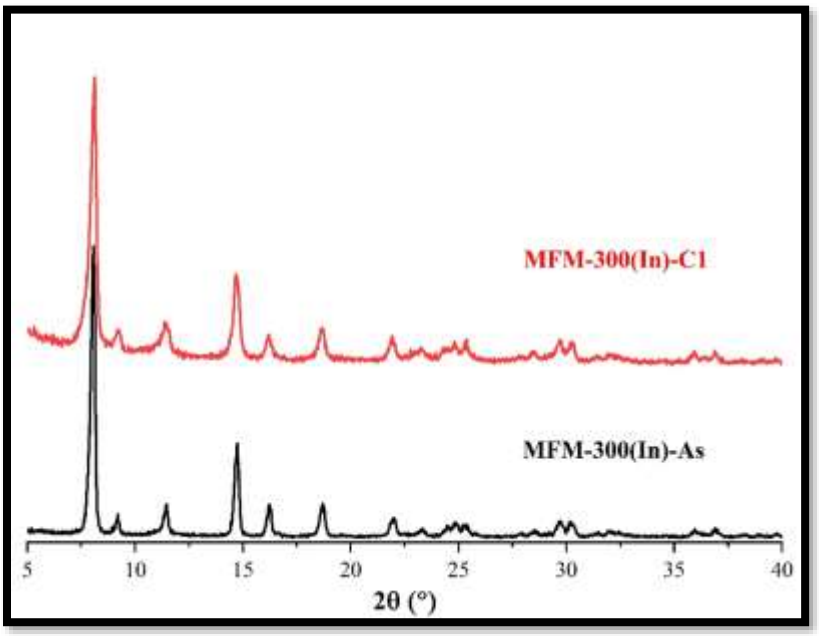

Figure S8. PXRD of MFM-300(In) after H_2S experiment (red) and as synthesised (black).

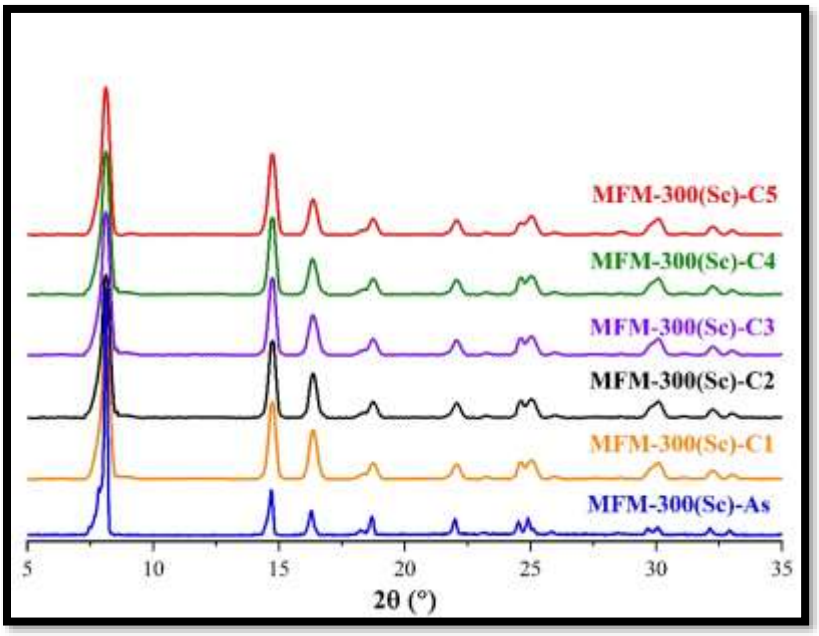

Figure S9. PXRD of MFM-300(Sc) for each H_2S cycle.

Thermogravimetric analysis (TGA)

TGA were performed in a TA Instruments Thermobalance, Q500 HR under N_2 atmosphere using the High-Resolution mode (dynamic rate TGA) with a rate of 5 °C/min, from room temperature to 650 °C.

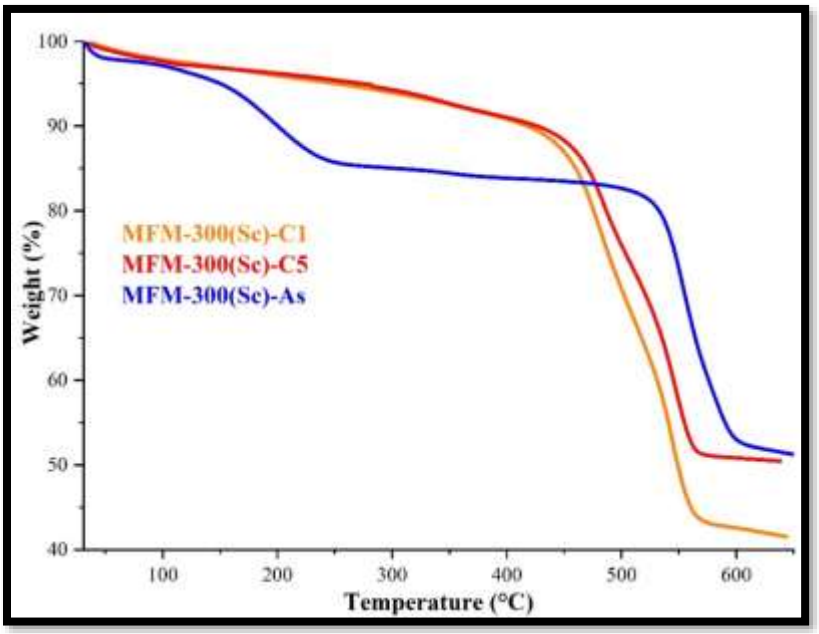

Figure S10. TGA of MFM-300(Sc) as synthesised (blue), 1 cycle (orange) and 5 cycles (red).

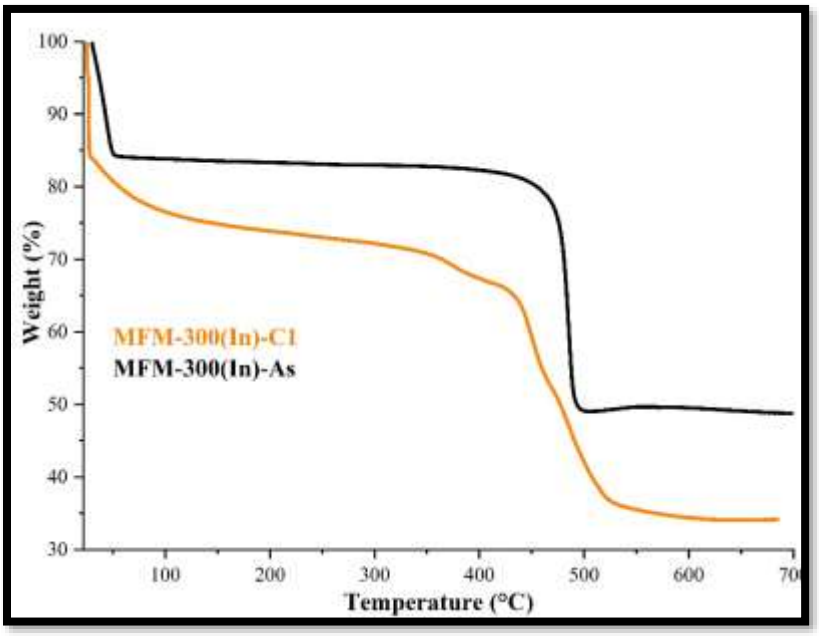

Figure S11. TGA of MFM-300(In) as synthesised (black) and 1 cycle (orange).

FTIR Spectroscopy.

FTIR spectra were measured (in-situ and at 25 °C) using an FTIR Nicolet 6700 spectrophotometer (DTGS detector) with a 4 cm^{-1} resolution equipped with a diffuse reflectance vacuum chamber with CaF_2 windows. FTIR spectra were collected on activated samples of MFM-300(Sc) and MFM-300(In) (8 x 10^{-6} bar and 180 °C for 2 hours). Pulses of CO, with an increment of 0.5 torr, were measured at N_2 liquid on activated samples.

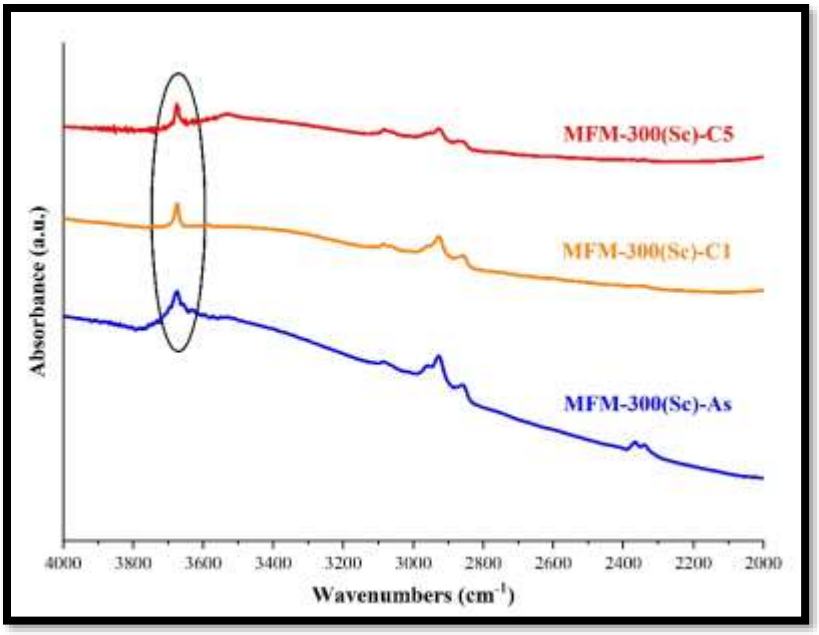

Figure S12. DRIFT spectra, after activation, of MFM-300(Sc) as synthesised (blue), 1 cycle (orange) and 5 cycles (red).

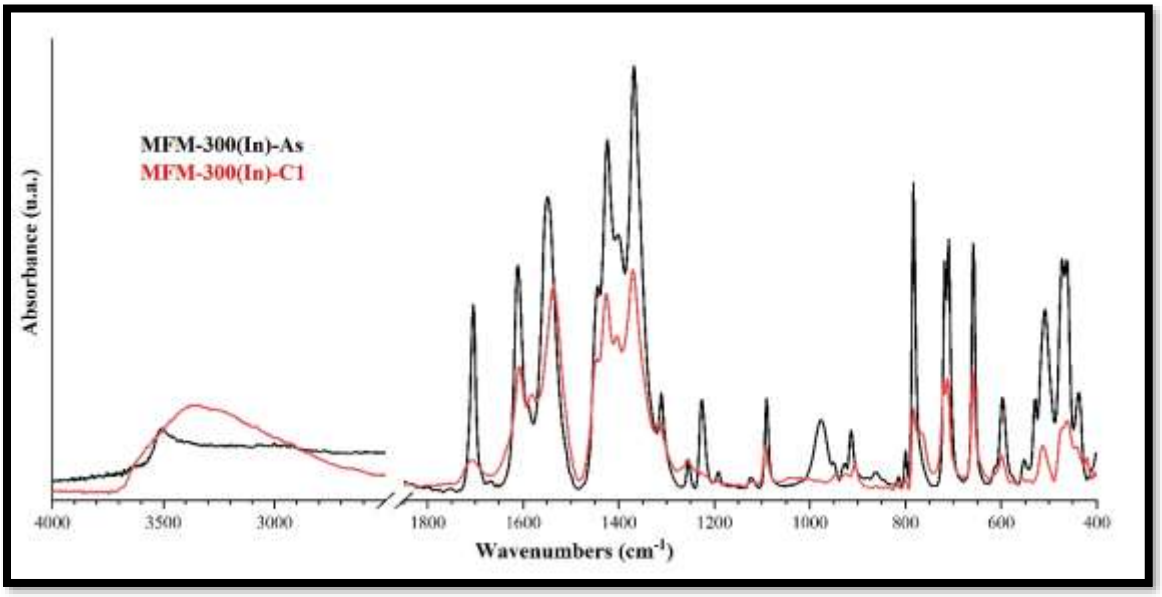

Figure S13. DRIFT spectra, after activation, of MFM-300(In) as synthesised (black) and 1 cycle (red).

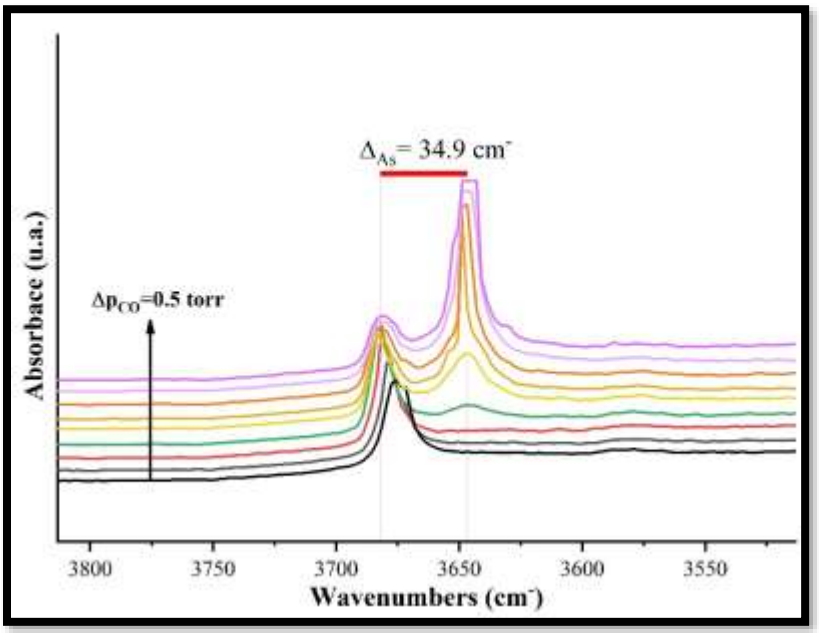

Figure S14. FTIR spectra of MFM-300(Sc) under a CO atmosphere at different CO pulses (by increment of 0.5 torr for each step or pulse).

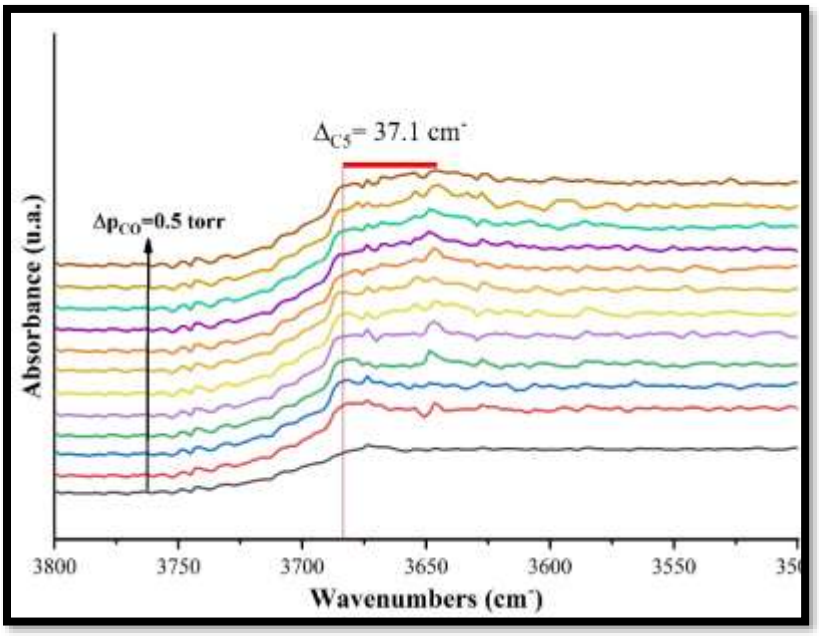

Figure S15. FTIR spectra of MFM-300(Sc) after 5 cycles of H_2S with CO pulses (increment of 0.5 torr for each step or pulse).

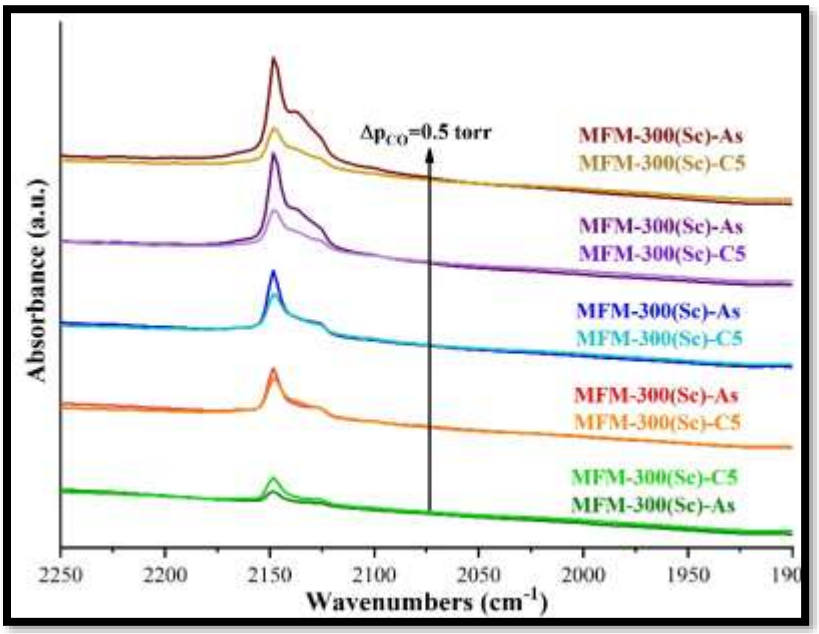

Figure S16. FTIR spectra of MFM-300(Sc) after 5 cycles of H_2S and as synthesised with CO pulses.

RAMAN analysis

The RAMAN experiments were measured on a DXR2 Thermo Scientific instrument with a lamp of 780 nm and 10X microscope objective for samples of MFM-300(Sc) and MFM-300(In) before and after H_2S experiments.

Figure S17. Picture of MFM-300(Sc) after 5 cycles of H_2S, with Raman microscope of 10x.

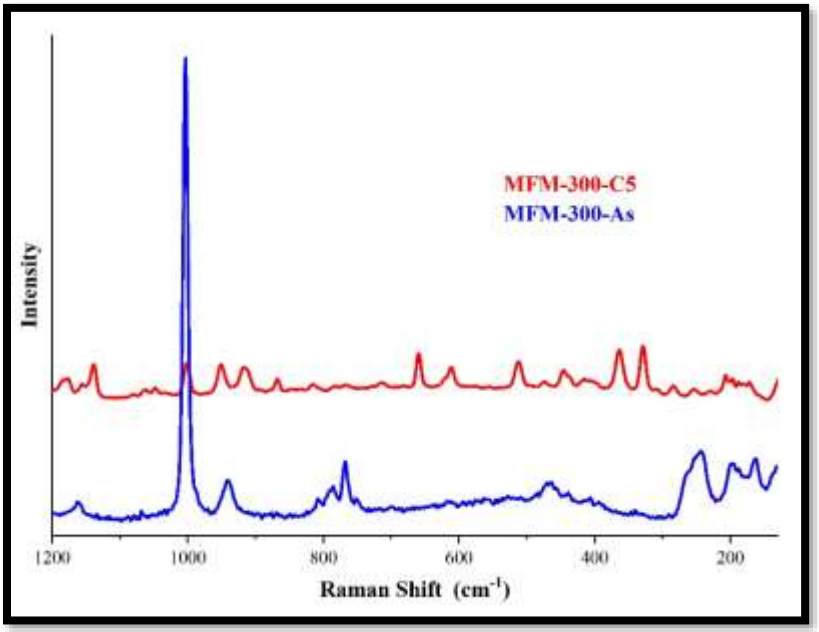

Figure S18. Raman spectra of MFM-300(Sc) after 5 cycles of H_2S (yellow zone from Figure S17) (red) and as synthesised (blue). The peaks observed in the 350-520 cm^{-1} region are associated to the S-S stretching vibrations modes of several polysulfides with various chain lengths.[5]

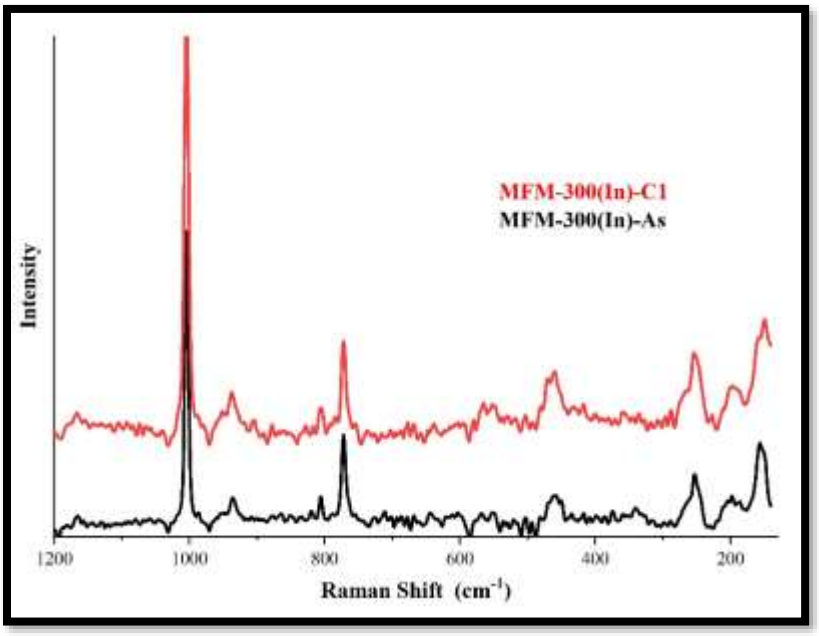

Figure S19. Raman spectra of MFM-300(In) after H_2S experiment (red) and as synthesised (black).

Scanning electron microscopy images (SEM)

SEM were recorded using a JEOL Benchtop Scanning Electron Microscope, Neoscope JCM-6000 using secondary electrons at 15 kV current in high vacuum.

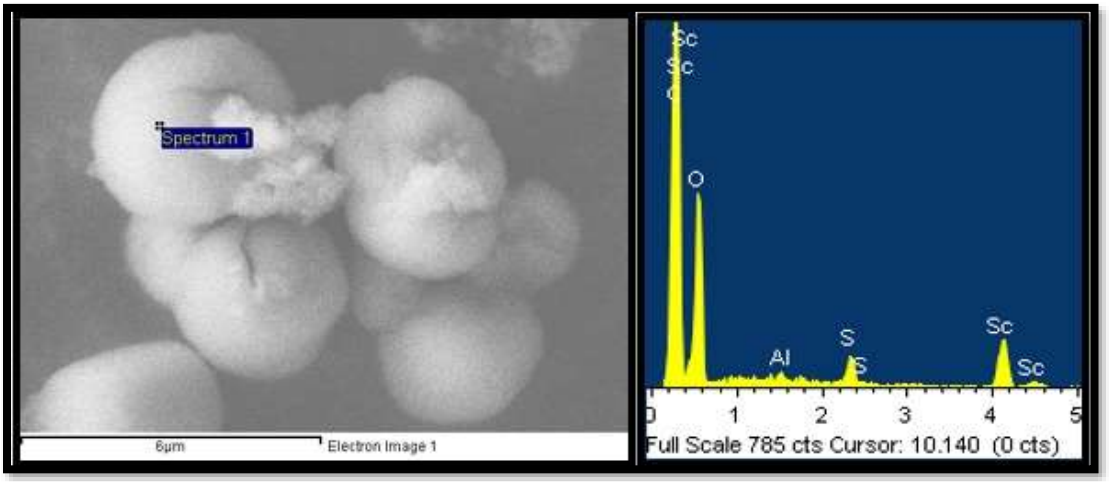

Figure S20. SEM picture and spectra of MFM-300(Sc) after 5 cycles of H_2S.

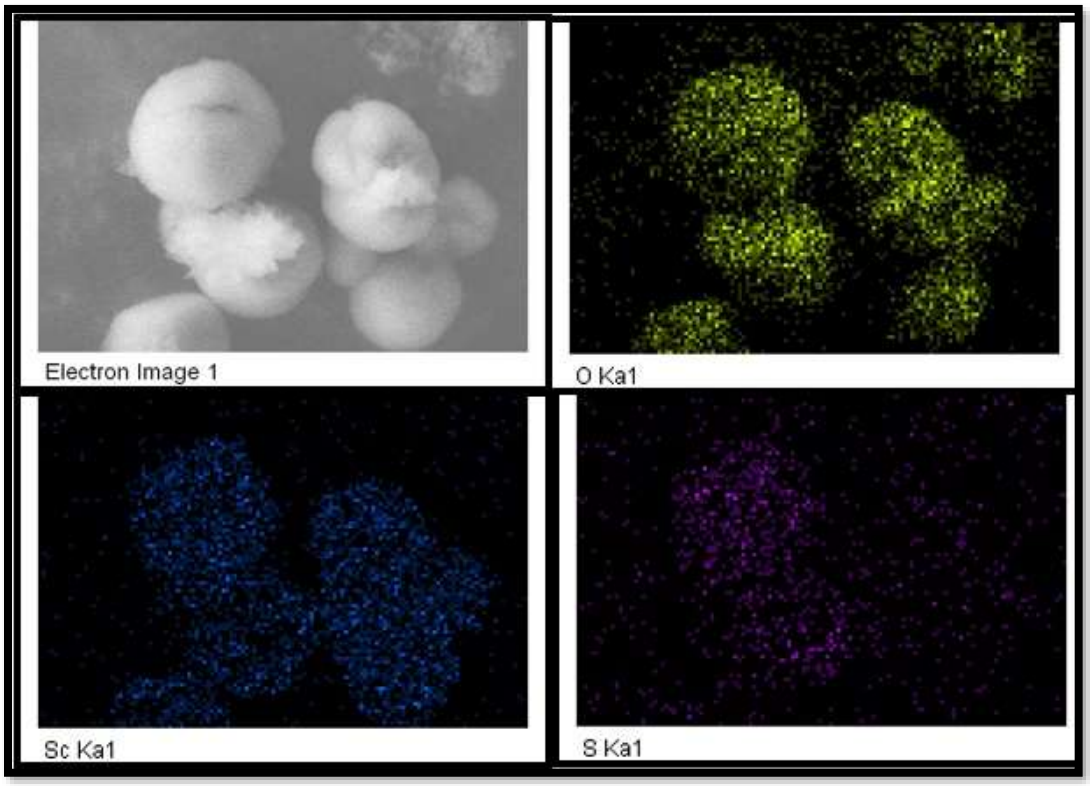

Figure S21. SEM mapping of MFM-300(Sc) after 5 cycles of H_2S. Up right: oxygen (yellow), down left: scandium (blue), down right: sulphur (purple).

Table S1. H_2S uptake in our system. *Breakthrough measurements using 6 %vol. H_2S/N_2 feed concentration and a 30 cm^3 min^{-1} flow rate.

Material	Uptake (mmol H_2S/g)	Reference
MFM-300(Sc)-C1	16.57	This work
MFM-300(Sc)-C2	10.08	This work
MFM-300(Sc)-C3	10.27	This work
MFM-300(Sc)-C4	10.21	This work
MFM-300(Sc)-C5	10.32	This work
MFM-300(In)-C1	9.1	This work
Al-MIL-53-TDC	18.13	6
MOF-74(Zn)	1.68*(1.64)	This work (7)
HKUST-1	1.12* (1.10)	This work (7)
MIL-101(Cr)	0.53* (0.40)	This work (7)

Table S2. Superficial area and H_2S uptake of MFM-300(Sc), one and two cycles.

Material	Superficial area BET and (pore volume)	Uptake (mmol H_2S/g)
MFM-300(Sc)-C1	1360 $m^2 g^{-1}$ (0.56 $cm^3 g^{-1}$)	16.53
MFM-300(Sc)-C1 re-activated at 25 °C for 2 h	898 $m^2 g^{-1}$ (0.37 $cm^3 g^{-1}$)	10.14
MFM-300(Sc)-C1 re-activated at 250 °C for 2 h	882 $m^2 g^{-1}$ (0.37 $cm^3 g^{-1}$)	10.32

Table S3. Amount of sulphur inside MFM-300(Sc) by elemental analysis.

Material	Weight of sulfur (%)
MFM-300(Sc)-As	0.01
MFM-300(Sc)-C1	0.11
MFM-300(Sc)-C5	4.10
STD Sulfanilamide (18.62%)	18.61

3. Electrochemical Characterization

The electrodes based on MFM-300(Sc), MFM-300(In) pristine and their analogues H_2S saturated labelled as H_2S@MFM-300(Sc) and H_2S@MFM-300(In) (equivalent to MFM-300(Sc)-C1 and MFM-300(In)-C1), as active materials were prepared according to the standard electrode preparation methodology for lithium-ion batteries [8]. In the first stage, 7 mg of polyvinylidene difluoride (PVDF) was dissolved in 0.2 mL N-Methyl-2-pyrrolidone (NMP) by magnetic stirring. Then, 7 mg of conductive carbon (CSP) was added and homogenized by magnetic stirring for 20 minutes, finally 86 mg of the pristine and H_2S saturated MOF type materials (MFM-300(M); M= Sc(III) and In(III)) were added and homogenised by magnetic stirring at 50 °C for 20 hours, to obtain homogeneous slurry. The MFM-300(M)CSP/PVDF cathodes were prepared by casting of slurry onto an aluminium foil by the doctor blade method to a 10 mm thickness. The resulting electrode was initially dried at 60 °C for 5 h in air atmosphere to vaporise the majority of the solvent and then. kept at 120 °C in a vacuum oven for 12 h in order to completely remove the solvent. All electrodes were prepared using a hot press roller at 80 °C with a 30 µm thickness separation, and then cut in the form of a circle of 18 mm diameter (2.54 cm^2 of area), and loading of active material (around 1.2 mg cm^2). The electrochemical characterisation was carried out using a two-electrode ECC-Combi electrochemical cell (EL-CELL) with metallic lithium as both the counter and the reference electrode, and glass fibber (Grade GF/F) from Whatman as a separator. The electrolyte used was 1 M LiTFSI in Triethylene glycol dimethyl ether (Triglyme). The cells were assembled inside an argon-filled glove-box (MBraun UNILab, H_2O and O_2 contents < 0.5 ppm). All the electrochemical measurements were performed using a Multi-Potentiostat/Galvanostat VMP3 from Bio-Logic Science Instruments.

Electrochemical potentials relevant for the identification of polysulfides in MFM-300(Sc and MFM-300(In).

$$S_8 + 2e^- + 2Li^+ \leftrightarrow Li_2S_8 \qquad > 2.3\,V$$

$$3Li_2S_8 + 2e^- + 2Li^+ \leftrightarrow 4Li_2S_6 \qquad > 2.3\,V$$

$$2Li_2S_6 + 2e^- + 2Li^+ \leftrightarrow 3Li_2S_4 \qquad 2.3\ to\ 2.1\,V$$

$$Li_2S_4 + 2e^- + 2Li^+ \leftrightarrow 2Li_2S_2 \qquad 1.9\ to\ 2.1\,V$$

$$Li_2S_4 + 2e^- + 6Li^+ \leftrightarrow 4Li_2S \qquad 1.9\ to\ 2.1\,V$$

$$Li_2S_2 + 2e^- + 2Li^+ \leftrightarrow 2Li_2S \qquad < 1.9\,V$$

Polysulfides formation from H_2S adsorbed

The formation of polysulfides from H_2S adsorbed can proceed through a sequence of steps: In the first part, H_2S is adsorbed within the MFM-300 materials (inside the pores) modifying the redox properties of H_2S. The mechanism can be explained as below, adapted from ref:[9,10]

I. *H_2S* adsorption at MOF surface: $H_2S(g) \rightarrow H_2S(ads)$

II. 2*H_2S*(ads) is dissociated:
$2H_2S(g) \rightarrow 2HS(ads) + 2H(ads)$

III. $2HS(ads) + 2H(ads) \rightarrow$ *S-S(ads) + 2H_2(g)* ↑

IV. Formation of linear or cyclic sulfur polymers (sulfur recombination):
XS-S(ads) → XS_x(ads)

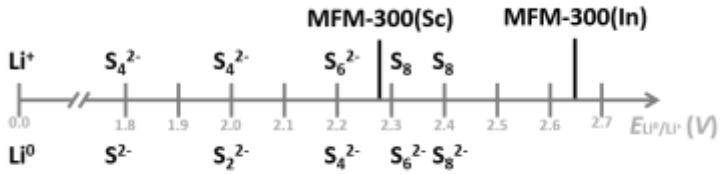

Scheme S2. Redox scale for the polysulphides species. Marking the initial OCP value for the MFM-300(M) electrodes (M= Sc(III) and In(III)).

$$S_8 + 2e^- \rightarrow S_8^{2-} \qquad \sim 2.4\,V$$

$$S_8^{2-} \leftrightarrow S_6^{2-} + \frac{1}{4}S_8$$

$$2S_6^{2-} + 2e^- \rightarrow 3S_4^{2-} \qquad \sim 2.1\,V$$

$$2S_4^{2-} \rightarrow S_2^{2-} + S_3^{2-}$$

$$S_4^{2-} + 6e^- \rightarrow 4S^{2-} \qquad \sim 2.0\,V$$

$$3S_2^{2-} \rightarrow S_4^{2-} + 2S^{2-}$$

4. Microscopic Models for MFM-300(Sc), H_2S and Interatomic Potentials.

Initial atomic coordinates for MFM-300(Sc) were taken from a previously reported study[1,2]. The Lennard-Jones (LJ) parameters for the organic and inorganic parts of MFM-300(Sc) were taken from DREIDING[11] force field and the UFF[12] force field respectively. The partial atomic charges for each framework atom of MFM-300(Sc) were extracted from periodic Density Functional Theory (DFT) calculations using the ESP[13] method as implemented in Dmol^3 and the PBE[14] functional and the DNP[15] basis set. The H_2S molecule was represented by the model reported by Kamath *et. al.*[16]. This corresponds to a rigid model with three charged sites centered in the atomic positions where only the S atom is a LJ interacting site, with a S-H bond of 1.34 Å and a H-S-H bond angle of 92.5°. The MFM-300(SC)/H_2S interactions were described using a 12-6 LJ potential and a coulombic contribution. Using a general approach adopted in previous studies,[17,18] the H atom from the μ-OH group and the Sc atoms interact with the guest molecules only through electrostatic interactions. LJ crossed parameters between the MOF material and the guest molecules were calculated with the Lorentz-Berthelot mixing rules. A cut off distance of 12 Å was used for the LJ contributions, while the long-range electrostatic interactions were handled with the Ewald summation technique[19,20].

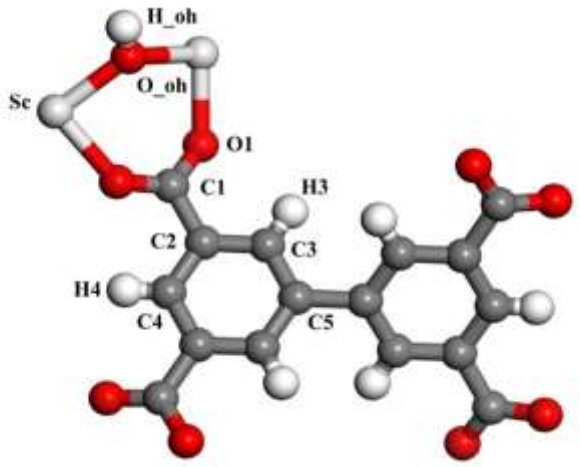

Figure S22. Labels of the atoms for the organic and inorganic parts of MFM-300(Sc).

Details of Monte Carlo Simulations.

A simulation box was made of 4 unit cells (2×2×1) while fixing all atoms of the framework in their initial positions. All MC simulations were performed using the simulation code

CADSS (Complex Adsorption and Diffusion Simulation Suite),[21] with the consideration of 2×10^7 cycles in each of the simulations.

MC simulations in the μVT ensemble were carried out at 298 K to predict the adsorption behaviour of H_2S as a single component in the range of 0.0001 to 20 bar. The fugacity used for each of the simulations was calculated using the Peng-Robinson equation.

Complementary MC simulations were carried out in the NVT ensemble to explore the preferential adsorption sites of H_2S as a single component at very low, low, intermediate and high loading. These studies involved the analysis of the radial distribution functions (RDFs) plotted between different MOF/guest atoms pairs averaged over hundreds of MC configurations. The adsorption enthalpies at low coverage were also calculated using the revised Widom test particle insertion[22].

Simulated H_2S adsorption isotherm.

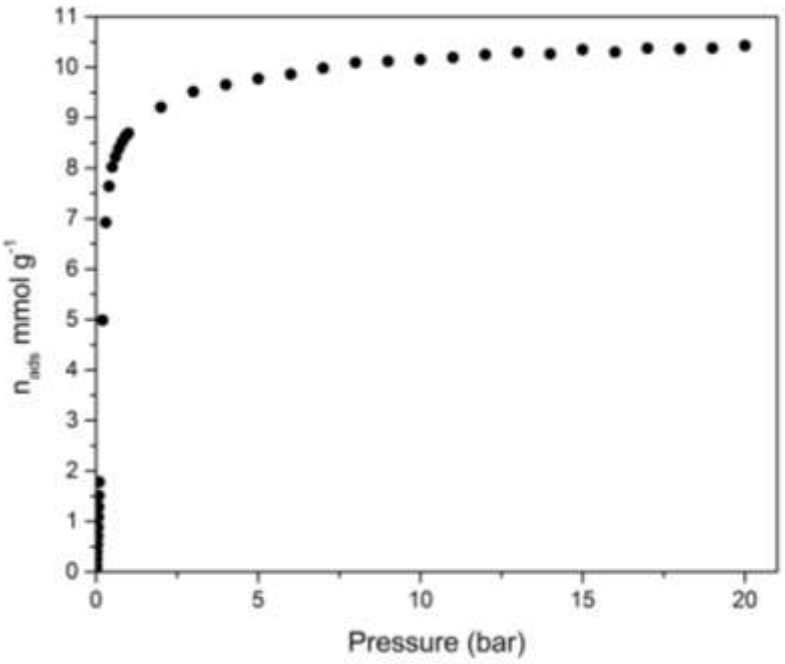

Figure S23. GCMC simulated adsorption H_2S isotherm as single component up to 20 bar at 298 K.

Simulated distributions of the H_2S molecules in the Pores

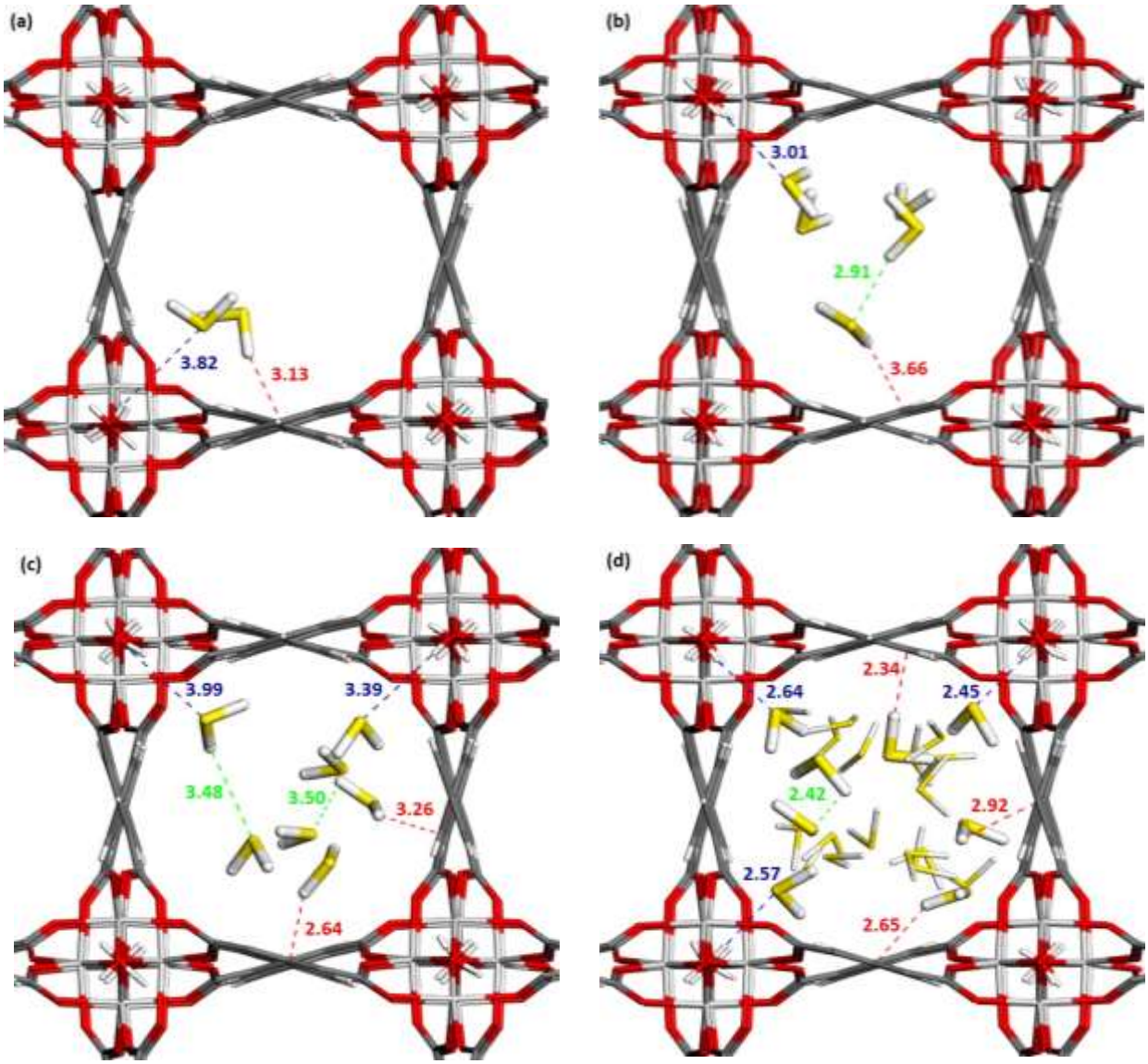

Figure S24. Snapshots extracted from MC simulations for different loadings of H_2S molecules (a) 2.70 molecules of H_2S per unit cell (b) 14.08 molecules of H_2S per unit cell (c) 28.17 molecules of H_2S per unit cell (d) 56.34 molecules of H_2S per unit cell. The distances are reported in Å. (Sc, light gray; O, red; S, yellow; C, grey; H, white). (Interaction (Dashes lines): S_{h2s}-$H_{\mu\text{-}OH}$(Blue), H_{h2s}-C_{org}(Red), S_{h2s}-H_{h2s}(Green)).

Radial Distribution Functions.

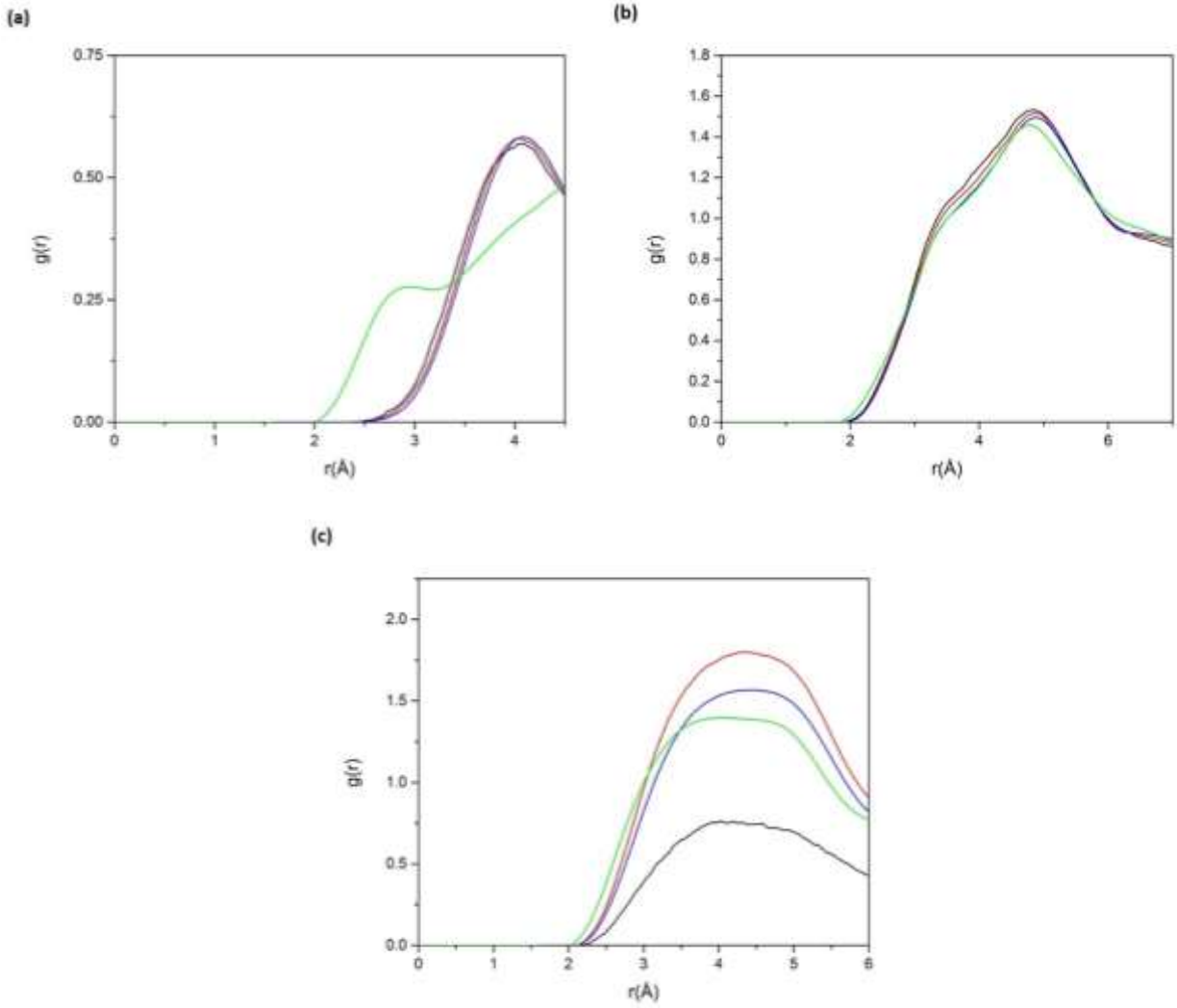

Figure S25. Radial distribution functions for the pair (a) S_{h2s}-$H_{\mu\text{-}OH}$, (b) C_{org}-H_{h2s} and (c) S_{h2s}-H_{h2s} at different loads of H_2S. (2.70 molecules of H_2S per unit cell, black; 14.08 molecules of H_2S per unit cell, red; 28.17 molecules of H_2S per unit cell, blue and 56.34 molecules of H_2S per unit cell, green).

References

(1) Ibarra, I. A.; Yang, S.; Lin, X.; Blake, A. J.; Rizkallah, P. J.; Nowell, H.; Allan, D. R.; Champness, N. R.; Hubberstey, P.; Schröder, Highly porous and robust scandium-based metal–organic frameworks for hydrogen storage. *Chem. Commun.* **2011**, 47, 8304-8306.

(2) Ibarra, I.A., Mace, A., Yang, S., Sun, J., Lee, S., Chang, J.S., Laaksonen, A., Schröder, M., and Zou, X. Adsorption properties of MFM-400 and MFM-401 with CO_2 and hydrocarbons: Selectivity derived from directed supramolecular interactions. *Inorganic Chemistry*. **2016**, *55*, 7219–7228.

(3) Qian, J.; Jiang, F.; Yuan, D.; Wu, M.; Zhang, S.; Zhang, L.; Hong, M. Highly Selective Carbon Dioxide Adsorption in a Water-Stable Indium-Organic Framework Material. *Chem. Commun.* **2012**, 48, 9696–9698.

(4) Nugent, P.; Giannopoulou, E. G.; Burd, S. D.; Elemento, O.; Giannopoulou, E. G.; Forrest, K.; Pham, T.; Ma, S.; Space, B.; Wojtas, L.; et al. Porous Materials with Optimal Adsorption Thermodynamics and Kinetics for Co2 Separation. *Nature* **2013**, 495, 80–84.

(5) Hagen, M.; Schiffels, P.; Hammer, M.; Dörfler, S.; Tübke, J.; Hoffmann, M. J.; Althues, H.; Kaskel, S. In-Situ Raman Investigation of Polysulfide Formation in Li-S Cells. *J. Electrochem. Soc.* **2013**, 160, A1205-A1214.

(6) Zárate, J. A.; Sánchez-González, E.; Jurado-Vázquez, T.; Gutiérrez-Alejandre, A.; González-Zamora, E.; Castillo, I.; Maurin, G.; Ibarra, I. A. Outstanding Reversible H_2S Capture by an Al(III)-Based MOF. *Chem. Commun.* **2019**, 55, 3049–3052.

(7) Liu, J.; Wei, Y.; Li, P.; Zhao, Y.; Zou, R. Selective H_2S/CO_2 Separation by Metal–Organic Frameworks Based on Chemical-Physical Adsorption. *J. Phys. Chem. C*, **2017**, *121*, 13249–13255.

(8) Guzmán, G.; Vazquez-Arenas, J.; Ramos-Sánchez, G.; Bautista-Ramírez, M.; González, I. Improved Performance of $LiFePO_4$ Cathode for Li-Ion Batteries through Percolation Studies. *Electrochim. Acta* **2017**, 247, 451–459.

(9) AN, S. The Reaction Mechanisms of H_2S Decomposition into Hydrogen and Sulfur: Application of Classical and Biological Thermodynamics. *J. Thermodyn. Catal.* **2017**, 08.

(10) Barchasz, C.; Molton, F.; Duboc, C.; Leprêtre, J. C.; Patoux, S.; Alloin, F. Lithium/Sulfur Cell Discharge Mechanism: An Original Approach for Intermediate Species Identification. *Anal. Chem.* **2012**, 84, 3973–3980.

(11) Mayo, S. L.; Olafson, B. D.; Goddard, W. A. DREIDING: A Generic Force Field for Molecular Simulations. *J. Phys. Chem.* **1990**, 94, 8897–8909.

(12) Rappe, A. K.; Casewit, C. J.; Colwell, K. S.; Goddard, W. A.; Skiff, W. M. UFF, a Full Periodic Table Force Field for Molecular Mechanics and Molecular Dynamics Simulations. *J. Am. Chem. Soc.* **1992**, 114, 10024–10035.

(13) Hamad, S.; Balestra, S. R. G.; Bueno-Perez, R.; Calero, S.; Ruiz-Salvador, A. R. Atomic Charges for Modeling Metal-Organic Frameworks: Why and How. *J. Solid State Chem.* **2015**, 223, 144–151.

(14) Perdew, J. P.; Burke, K.; Ernzerhof, M. Generalized Gradient Approximation Made Simple. *Phys. Rev. Lett.* **1996**, 77, 3865–3868.

(15) Hehre, W. J.; Ditchfield, R.; Pople, J. A. Self—Consistent Molecular Orbital Methods. XII. Further Extensions of Gaussian—Type Basis Sets for Use in Molecular Orbital Studies of Organic Molecules. *J. Chem. Phys.* **1972**, 56, 2257–2261.

(16) Kamath, G.; Lubna, N.; Potoff, J. J. Effect of Partial Charge Parametrization on the Fluid Phase Behavior of Hydrogen Sulfide. *J. Chem. Phys.* **2005**, 123.

(17) Damasceno Borges, D.; Normand, P.; Permiakova, A.; Babarao, R.; Heymans, N.; Galvao, D. S.; Serre, C.; De Weireld, G.; Maurin, G. Gas Adsorption and Separation by the Al-Based Metal-Organic Framework MIL-160. *J. Phys. Chem. C.* **2017**, 121, 26822–26832.

(18) Sánchez-González, E.; Mileo, P. G. M.; Sagastuy-Breña, M.; Álvarez, J. R.; Reynolds, J. E.; Villarreal, A.; Gutiérrez-Alejandre, A.; Ramírez, J.; Balmaseda, J.; González-Zamora, E.; et al. Highly Reversible Sorption of H_2S and CO_2 by an Environmentally Friendly Mg-Based MOF. *J. Mater. Chem. A* **2018**, 6, 16900–16909.

(19) Osychenko, O. N.; Astrakharchik, G. E.; Boronat, J. Ewald Method for Polytropic Potentials in Arbitrary Dimensionality. *Mol. Phys.* **2012**, 110, 227–247.

(20) Kolafa, J.; Perram, J. W. Cutoff Errors in the Ewald Summation Formulae for Point Charge Systems. *Mol. Simul.* **1992**, 9, 351–368.

(21) Yang, Q.; Liu, D.; Zhong, C.; Li, J.-R. Development of Computational Methodologies for Metal–Organic Frameworks and Their Application in Gas Separations. *Chem. Rev.* **2013**, 113, 8261–8323.

(22) Vlugt, T. J. H.; García-Pérez, E.; Dubbeldam, D.; Ban, S.; Calero, S. Computing the Heat of Adsorption Using Molecular Simulations: The Effect of Strong Coulombic Interactions. *J. Chem. Theory Comput.* **2008**, 4, 1107–1118.